Proc. Natl. Acad. Sci. USA
Vol. 77, No. 3, pp. 1447–1451, March 1980
Biophysics

Magnetic fields produced by steady currents in the body

(steady magnetic field/direct current/steady potentials/hair follicle)

DAVID COHEN*, YORAM PALTI†, B. NEIL CUFFIN*, AND STEPHEN J. SCHMID*‡

*Francis Bitter National Magnet Laboratory, Massachusetts Institute of Technology, Cambridge, Massachusetts 02139; †Department of Physiology and Biophysics, Technion Medical School, Haifa, Israel; and ‡Hughes Aircraft Corporation, El Segundo, California

Communicated by Benjamin Lax, December 14, 1979

ABSTRACT **The magnetic fields produced by naturally occurring steady currents in the body were measured by using a new magnetic gradiometer in a magnetically shielded room. A field of 0.1 μG/cm with reproducible pattern was seen over the head and over the limbs, whereas the field over the torso proper was weaker (except over the abdomen). Most of the field over the head is produced by electrical sources associated with the hair follicles of the scalp; this field is produced only as a response to touching or pressing the scalp, in regions where the hair is dense. Most of the field over the limbs is produced by electrical sources associated with the muscles. The field over the forearm, studied in detail, was often present spontaneously; when absent, it could be induced by mild twisting and rubbing. On the basis of auxiliary experiments involving electrolytes, a general mechanism for generation of steady current in the body is suggested. In this mechanism, the steady current is generated by a nonclosed or a nonuniform polarized layer across an elongated semipermeable membrane such as a muscle fiber; the nonuniform polarization is due to a gradient of extracellular K^+ along the membrane.**

During the past 15 years or so, magnetic fields produced by the human body have been measured (1, 2). These fields are very weak, in the range of 10^{-10} to 10^{-5} gauss (G), and are measured with the sensitive magnetic detector called the SQUID (superconducting quantum interference device) (2, 3). The body's fields are produced either by naturally occurring electric currents in the body or by contaminating ferromagnetic particles. The electric currents, which consist of the flow of ions, can be either fluctuating current or steady current; steady current is here called dc current (dcI) and refers to frequencies <0.1 Hz. Most of the body's fluctuating magnetic fields, such as those from the heart or the brain produced by the same currents that produce the electrocardiogram and electroencephalogram, have already been studied (2). We are here concerned with the dc magnetic field (dcMF) produced by the dcI. Up to now some dcMFs have only been briefly noted; these are the dcMFs over the abdomen (4, 5), upper arm (6), chest (5), and eyes (7). We present here a more detailed study and mapping of the body's dcMF, including a dcMF over the head from an unexpected source.

The dcMF can be important for two reasons; both involve comparison of the dcMF with the dc potential (dcP) produced by the same source in the body. First, as will be shown, there need be no dcMF produced by a source that produces a dcP; stated otherwise, the dcMF is produced only by a subgroup of the sources that produce the dcP. Measurements of the dcMF can therefore be a new, specialized probe of the dc sources in the body. The second reason is that measurements of the dcMF appear to be a more reliable way of determining the dc source in an internal organ than measurements of the dcP it produces on the skin. Whereas this dcP measurement is known to be difficult or impossible because of interfering dcPs generated in the skin, mostly by the sweat glands, the dcMF is subject to much less interference by the skin; this is probably because the sweat glands are perpendicular to the skin surface, later explained to be an orientation producing no dcMF. Although we show here that a dcMF can indeed be produced by a special region of the skin, namely the scalp, the remainder of the body's skin appears to produce no interfering dcMF.

The main problem in measuring the dcMF has previously been the low-frequency magnetic background due to elevators, trucks, etc. Our design and use here of a new SQUID system, called the 2-D detector, greatly decreases this problem; it also allows a simple visual display of the dcI that produces the dcMF. With this system we have been able to conveniently map the dcMF over the entire body, and to make extensive measurements over the human head and forearms in particular. To gain information about the sources producing these dcMFs we made auxiliary experiments and observations. For the human body not only did these include manipulations such as the application of pressure, cooling, etc., but these include also the injection of electrolytic solutions into muscle regions in order to assess the role of polarized membranes in producing the dcMF; a wider range of injections was made in an anesthetized dog. In addition, to assess the role of liquid junctions as sources, measurements were made of the dcMF produced by models consisting of compartments of different electrolytes in contact.

MATERIALS AND METHODS

The 2-D detector used here consists of two separate SQUID channels; each is a complete gradiometer. These are both located in the tail of a liquid helium dewar that is mounted in the Massachusetts Institute of Technology shielded room as previously illustrated (2, 6). A measurement of the dcMF produced by any source, for example a dcI in a wire or in part of the human body, is made by bringing that source up close to the tail, which remains stationary. During the approach of the source, the dcMF induces a signal in a superconducting "antenna" coil of each channel shown in Fig. 1*A*. The subsequent SQUID and electronics of each channel convert this signal to yield a final output voltage proportional to $\Delta B_z/\Delta x$ or $\Delta B_z/\Delta y$, the gradient of the dcMF at the detector; the frequency response is flat down to dc. The output voltage, therefore, depends only on the position of the source, not on the rate of change. When a B_z-coil detector (Fig. 1*B*) was used in our shielded room (2), the magnetic background interfered with dcMF measurements (the low frequencies can penetrate the shielding); however, there is usually no interference when the 2-D system is used in the shielded room. This is because the close spacing of the Ds D-shaped coils in Fig. 1 makes each 2-D coil insensitive to the almost uniform field from a distant source.

When an x–y scope is fed by the outputs, as in Fig. 1*D*, it makes a most useful "arrow" display of the source current.

The publication costs of this article were defrayed in part by page charge payment. This article must therefore be hereby marked "*advertisement*" in accordance with 18 U. S. C. §1734 solely to indicate this fact.

Abbreviations: SQUID, superconducting quantum interference device; dcI, steady current; dcMF, dc magnetic field; dcP, dc potential; VC, volume conductor; emf, electromotive force.

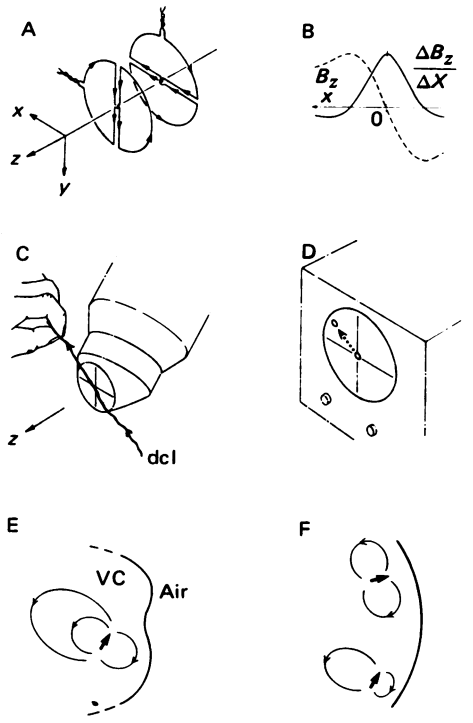

FIG. 1. The 2-D detector and some sources. (*A*) The two "antenna" coils, 2.8 cm in diameter, with exaggerated z-separation. Each coil consists of two Ds; each D responds to B_z, the z-component of the magnetic field vector $\vec{B}$. Because the two Ds are connected in opposition, each coil responds to ΔB_z, the difference in B_z between the Ds. The response of the front coil is proportional to the gradient $\Delta B_z/\Delta x$ and that of the rear coil, to $\Delta B_z/\Delta y$, where Δx or Δy is the mean separation between the Ds. (*B*) The response of both the $\Delta B_z/\Delta x$ coil and the B_z coil we had used previously (simple loop of the same diameter) to a test wire carrying current in the y direction, as a function of the wire's x-position. The 2-D coil response is maximal when the test current is at the coil midline, in contrast to the B_z coil where the maximum is at an x-location greater than the coil radius; therefore one advantage of the 2-D coil is to locate easily a line current, namely at its midline. (*C*) The two coils (decreased scale) in use, now located 0.7 cm behind the cross-hairs, in the tail of a liquid-helium dewar. Each is connected to a SQUID higher in the tail. The outputs of the two channels feed the x and y inputs of the scope in *D*. When a test wire is brought up to the tail, as in *C*, the spot on the scope moves from the screen center to the upper left, making an arrow having the direction and magnitude of the wire's dcI. (*E*) Distributed dcI in a biological object of arbitrary shape. The dcI consists of both a source current (heavy arrow representing a current dipole) and the current generated in the VC by this dipole, called the volume current (light lines). The scope arrow would mimic the x–y projection of both. (*F*) Two different sources in a VC of spherical shape. The upper dipole is oriented radially to the surface, the lower dipole, tangentially. The detector cannot see the upper source. For the lower source, the arrow would mimic only the dipole; its volume current cannot be seen.

When the source is the test wire of Fig. 1*C*, the scope spot makes an arrow that simply mimics the dcI in the wire. However, when the source is in the body, the dcI is distributed in the volume conductor (VC) of the body as in Fig. 1*E*; the scope arrow then mimics the dcI in the detector field of view, which includes both source and volume current. A pattern of arrows mapped over a surface of the body therefore roughly duplicates the pattern of underlying flow of dcI, both source and volume current. There is a simplification if the VC surface is either spherical, as in Fig. 1*F*, or planar. In those cases it can be shown (9) that a radial (or normal) dipole and its currents produce zero external dcMF, and only the tangential source produces a dcMF. Further, only the tangential dipole itself, not its volume current (8), produces the dcMF we measure (the B_zs). Skin of almost any shape can be considered to be a planar surface for sources within it, because the source–surface separation is small compared to the skin's radius of curvature.

The two 2-D outputs were monitored on the x–y scope and recorded on a two-channel chart recorder. Whenever more extensive off-line analysis was required, the signals were also tape-recorded for later playback. The only dcMF artifact originated from contamination of the body surface by ferromagnetic particles; this was eliminated by thoroughly cleaning and demagnetizing the areas involved; also, the dog was shaved. Rare failures of these precautions could be readily detected as sharp, irregular signals as the body surface was scanned.

Two electrolytic liquid-junction models were used. The first consisted of a horizontal triangle of glass tubing (1.6 cm internal diameter). The three compartments, each ≈25 cm long, were filled with three solutions that were separated at the apices by stopcocks; three junctions were thus formed by opening the stopcocks. In additional experiments two solutions (two junctions) were also used. The junction electromotive forces (emfs) generated a net dcI around the loop, producing a dcMF that was measured by sliding the triangle up to and away from the detector. This dcMF was compared with that seen over the body. From the dcMF the dcI was calculated, which, multiplied by the ac resistance of the loop (measured with electrodes), gave the junction emfs for any future considerations. The second model, designed to better approximate the mixing and diffusion in the body, consisted of a disc-shaped container (7 cm in diameter) of saline (0.165 M) gel. One or more 1-ml boluses of electrolytes could be injected into the gel to form various junctions, and the resulting dcMF was measured as with the triangle.

RESULTS

Natural dcMFs. Reproducible dcMFs were measured over the human head and limbs. Almost all the dcMF over the head was produced only as a result of pressing on the scalp, however lightly; this was usually done by touching the head against the dewar tail. This "touch-dcMF" was always present over any scalp area containing hair, with a distinct arrow pattern shown in Fig. 2; also, it was usually present over the hairy areas of the male face. It was always absent over areas devoid of thick hair, such as the forehead, cheeks, or bald pates (which have only vellus hair). The subjects included 15 full-haired young men, 2 middle-aged men with thinning hair, and 4 men who were top-bald. Increasing age, say from 20 to 60 yr, decreased the amplitude by a factor of 2 or more, but with no direction change. The pattern remained constant under exercise (15 min), body inversion (feet up, head down), and demagnetizing; it also remained constant after the application of a magnetizing field, electrically conducting paste, and hot packs to the scalp. However, cold packs could produce a 50% amplitude increase. There was a simple arrow pattern over the head of the single dog we used, with amplitude of ≈100 nG/cm; however the dependency on touch is not known. After a fatal dose of sodium pentobarbital, this pattern remained constant for 10 min after circulation ceased, then during the next 30 min the arrows changed directions.

The dcMF over the forearm (five normal male subjects) was in the range of 50–150 nG/cm; the other limb areas showed the same range, except over the leg it was larger, up to 300 nG/cm. The field over the forearm was often present spontaneously; when absent it could always be induced by repeated mild twisting or rubbing of the forearms, not by touching. Although the arrow pattern was symmetric in left and right arms and was reproducible from day to day for any individual, it varied greatly among individuals, unlike the head pattern; two examples are shown in Fig. 3. Generally the arrow directions changed after application of hot, cold, and a tourniquet for

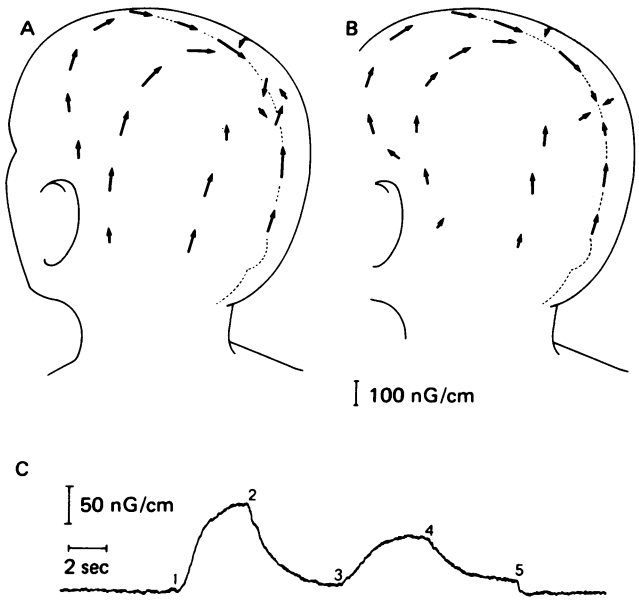

FIG. 2. (*A* and *B*) Arrow patterns of the touch-induced dcMF over the scalp of two full-haired young men. The dotted line is the midline of the scalp. The pattern is similar for all full-haired subjects and is always left–right symmetric, except for a whorl on the midline, as in *A*. The scale bar refers to the arrow length, which gives the amplitude of the field gradient. For all subjects the maximal amplitude is in the range 100–250 nG/cm; 100 nG/cm would be produced by a dipole of strength 1.0 μA-cm or an infinite wire carrying 0.5 μA, both at 1.0 cm from the coils, which is at the depth of the subcutaneous layer of the scalp. (*C*) Typical time course of the dcMF, from a head location above the inion (bump). Because the arrow is vertical there, only the tracing from the nonzero SQUID channel ($\Delta B_z/\Delta x$) is shown. The head, which has been moved up to the dewar tail, touches it lightly but constantly at point 1. The resulting field grows until point 2, where the head is moved slightly away from the tail and held fixed. With no pressure, the signal decreases until point 3 where the head again touches the tail. At point 4 the touch is again relieved, and at point 5 the head is moved out of range. The rise time is seen to be shorter than the decay time. With repeated touching the rise time increases and amplitude decreases by 1:2. When the scalp is firmly pressed after repeated touching, the amplitude increases to the first-touch level and the decay time decreases after pressure release. Although the rise time varies among subjects by 2-fold at most, the spread in decay times is about 6-fold.

several minutes, and repeated flexing of any part of that limb. Three polio victims were measured, each with one normal arm and the other of normal bone length but lacking muscle and nerve; for each victim, the normal arm showed normal arrow amplitudes, whereas the abnormal arm showed no dcMF.

The dcMF over the human torso proper (twelve normal adult males), including the especially muscular areas (pectoral, gluteal, etc.) was usually <30 nG/cm except at two regions; over the abdomen it was 100–1000 nG/cm depending on gastrointestinal activity (4), and over the scapulae it was ≈50 nG/cm. However, one wiry subject showed ≈100 nG/cm over the scapulae and parts of the chest, as did a boy (8 yr) whom we measured. There was no measurable touch-dcMF at the hairy underarm or pubic areas. Over both the normal female breast (six subjects) and over two different advanced breast tumors the dcMF was essentially zero.

Electrolytically Induced dcMFs. The injection into muscle areas of solutions containing more than 3–5 mM KCl, the normal extracellular K^+ concentration, will depolarize the muscle cell membranes in these areas; the remaining polarized section of each fiber should then act as a source of dcI. The injections, both subcutaneous and intramuscular, consisted of 0.5–1.0 ml of isotonic mixtures of KCl and NaCl. dcMFs could be induced by these injections only in areas where it was found naturally.

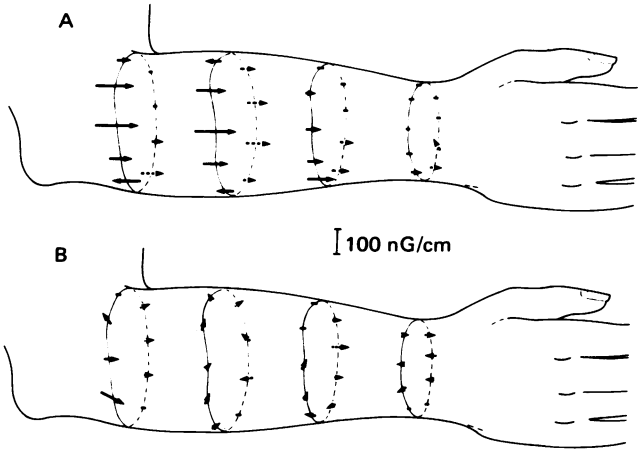

FIG. 3. Arrow pattern over the forearm of two normal subjects. Solid arrows are over the outer (viewer's) side of the arm and broken arrows are over the inner side. The patterns are characteristic of these subjects and indicate the wide variation from subject to subject. The dcMF of *A* was often absent, and the pattern shown could always be induced by 30 sec of light twisting and rubbing against the dewar tail. The pattern of *B* was usually present without this manipulation. Although *A* has a 6-cm length of scar tissue (scald) encircling the right forearm, the left and right forearm patterns are similar.

Specifically, the subcutaneous injection of isotonic 70 mM KCl (mixed with 95 mM NaCl) into the human forearm, 7–10 cm from the elbow, resulted in an amplitude increase over the injection site by a factor of 3–8, with variable pattern. The same injection into the upper pectoral region doubled the small natural field (from 15 to 30 nG/cm), whereas a 2-cm-deep injection into the gluteal region or subcutaneously into a woman's breast produced no change in the zero dcMF over these regions.

Control injections (zero volume or isotonic NaCl) into the dog thigh, which do not depolarize membranes, produced no change in the natural dcMF. Similarly, a subcutaneous injection of hypertonic NaCl (0.95 M), which produces only small depolarization of cells, produced almost no field change. In contrast, a subcutaneous injection of 0.3 M KCl, which strongly depolarizes the fibers, raised the dcMF to 800 nG/cm, whereas the even stronger 3.0 M KCl raised it to 3600 nG/cm. The time course of the dcMF due to this injection is shown in Fig. 4. The same bolus, injected deeper and intramuscularly, yielded a much smaller increase after correction for distance.

Liquid-Junction dcMFs. Generally, in two-junction circuits the emfs tend to cancel except for differences in mixing and therefore are smaller than in three-junction circuits. Thus, in the glass triangle system, two unrealistically strong solutions, 0.5 M NaCl and 3 M HCl, yielded a dcMF of 20 nG/cm (net

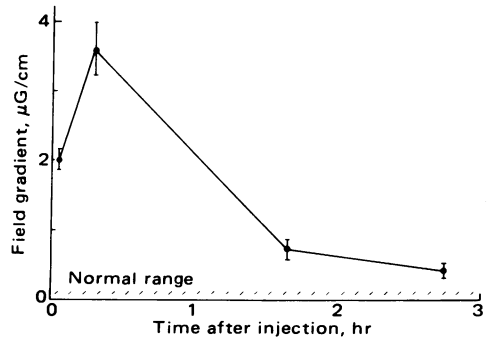

FIG. 4. The dcMF over the thigh of a dog, after subcutaneous injection of 0.5 ml of 3 M KCl at 0-time. The field gradient is seen to increase by a factor of about 60 from the normal (preinjection) level, measured to be in the range 40–70 nG/cm.

emf = 0.2 mV); also 0.5 M NaCl and 0.7 M KCl yielded 8 nG/cm (0.15 mV). One extreme set of three solutions, 0.17 M NaCl, 0.5 M NaCl, and 70 mM KCl, yielded 8 nG/cm (0.5 mV); also 0.17 M NaCl, 70 mM KCl, and 0.7 M KCl yielded 20 nG/cm (1.0 mV). The three-junction dcMFs were not higher because of the larger circuit resistance for these specific cases. Compared with the same solutions in the triangle system, the electrolytic gel arrangement in the disc yielded a large increase of dcMF. Thus, a 1-ml bolus of 3 M HCl injected into the saline gel yielded 200 nG/cm, whereas in a three-solution system a bolus of 0.7 M KCl in contact with another of 70 mM KCl yielded 80 nG/cm transiently, before settling to a lower, steady level. From these dcMFs, the maximal dcMF that natural liquid junctions in the body can produce is estimated to be 4 nG/cm; this is 1/30th of that measured at the head or limb. The estimate is based on more realistic ion concentrations and spacings.

DISCUSSION

We first discuss some basic aspects of dcI in the body, then apply these in interpreting the measured dcMFs. A biological source of dcI can always be characterized by a separation of charges. This separation produces a dcP in the VC, and the gradient of the dcP in turn produces a dcI; the dcI consists of the flow of all the positive and negative ions that make up the VC. For our purposes we assume the separated source charges to exist in the form of polarization across a boundary, as in Fig. 5*A*. In a physiological system this polarization is associated with an ion concentration difference across the boundary. The boundary may consist of a semipermeable membrane; in this case the emf across the membrane (hence polarization charge density) is related to the concentration differences via the Goldman equation (10) and its modifications, which reduces to the Nernst equation (11) when there is only one permeable ion and no pumps. Instead, the boundary may have no membrane and only be the junction between two liquids of different ion concentrations; the emf is then given by the liquid-junction equation (12). Phenomena other than these two that can produce source polarization, such as the streaming potential, appear to yield dcIs that are insignificant here.

All polarization layers will always produce a dcP, with one exception. This is the well-known, closed, uniformly polarized layer that gives dcP = 0 everywhere in the VC (13); hence for the production of a dcP, also its gradient and a dcMF, it is at least necessary that the layer not be closed, or be closed but polarized nonuniformly. However, although they produce a dcP, there are two classes of layers that produce no dcMF because of the geometry. Fig. 5*B* shows two examples in the first class; these are layers that produce a dcP but no dcI. An example of the second class is the radial dipole in Fig. 1*F*; here there is a dcI but no dcMF. These considerations illustrate the important fact that the dcMF is produced only by a subgroup of the sources that produce the dcPs.

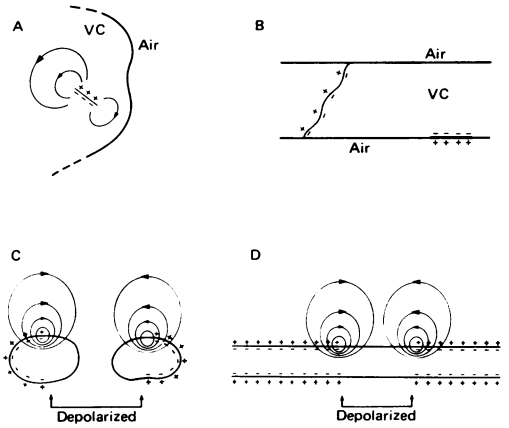

FIG. 5. (*A*) Separated charges in the form of a section of polarized layer, acting as a source of dcI in the VC. Any diffuse or nondiscrete separation of charges can be considered to be a continuum of these layers in series. (*B*) Examples of polarized layers that produce dcP but no dcI. The dcI has been interrupted by the insulator (air). The VC is here of cylindrical shape. The left layer is uniformly polarized and produces a uniform but different dcP on each side. The layer at the lower right can be nonuniform and produces a uniform dcP in the VC. (*C*) A depolarized region in a group of "spherical" cells. The polarized portions can only sustain a transient current, not dcI. (*D*) A depolarized region in a long, uniformly polarized cell or fiber. The polarized portion can generate a current of long duration.

With regard to the ion concentration differences, we will accept the fact that they exist in all living systems, and not be concerned with how they are produced in the body. However, these concentrations need to remain constant enough, and resist depletion by the current they generate, in order for this current to be steady and be called dcI. From this point of view there is considerable difference between the group of spherical cells shown in Fig. 5*C* and the long cylindrical cell or fiber in Fig. 5*D*. Although each type is shown with a depolarized region and therefore is able to generate a current, it can be deduced (14) that in partly depolarized spherical cells the ionic concentration differences vanish because of diffusion in a few seconds at most; hence their polarization disappears. In contrast, in Fig. 5*D* the long reservoir of ions, mainly K^+, can maintain the polarization (hence dcI) for many minutes. For example, calculations (14) were performed for an open-ended fiber of length 0.2 cm that show that the internal K^+ concentration drops by one-half in about 10 min (independent of diameter); the polarization changes accordingly. This time is more than 1 hr when length is 1.0 cm. Further calculations (unpublished results) show this time to be about 0.3 sec for a spherical cell of 30 μm diameter.

In discussing the measured dcMFs, we first consider the relative roles of membranes and liquid junctions. The data from the models, especially the gel, tend to rule out simple liquid junctions as responsible for dcMFs of the body. This conclusion is supported by the negative result of the K^+ injection into the muscle-free female breast; if liquid junctions produced a dcMF, it should have been seen in this case. The semipermeable membrane is then the only candidate for dcMF production; our data generally support this, especially the high fields induced by K^+ injection into a muscle area.

Considering next the touch-dcMF of the head, the source must certainly be in the skin because of the response to light touch. Because the scalp surface is relatively planar, the arrows of Fig. 2 indicate only source currents (no volume currents). The source must involve the thriving hair follicles, not only because this dcMF is absent where these follicles are absent, but also because the general arrow pattern (Fig. 2) was found to coincide with the common tilt pattern of the hair follicles of the scalp (15, 16); this includes the occasional whorl (Fig. 2*A*). Stated otherwise, the arrows coincide with the projection of the follicles onto the scalp surface; the arrows point "into" the follicles. The source associated with each follicle can therefore be considered as a current dipole pointing along the follicle into the root and located either within or near the follicle. If within, then this source could be, for example, equivalent to a polarized layer lining the follicle, with negative charges on the inside.

In attempting to understand the mechanism of the touch-dcMF, we have looked for its dcP equivalent in the literature. Although a touch-dcP has been seen and studied (17), it was seen in hairless areas such as under fingernails. Hence hair follicles are not involved and the phenomenon appears to be different from ours. We can find no published report of potentials associated with hair follicles. At this stage we can

therefore only guess at a mechanism. Perhaps there is a reflex whereby the touch stimulates the especially thick innervation surrounding each scalp follicle (18); this then produces a circulatory change and hence an ion concentration change at some elongated semipermeable membrane associated with the follicle. The remote possibility that the source involves a ferromagnetic entity at the follicle is ruled out by the negative results of magnetizing and demagnetizing.

That an electrical source associated with the hair follicle is seen by magnetic measurement, and not previously noted in various measurements of the dcP on the scalp (19, 20), is due to the fact that the dcMF is produced only by a subgroup of the generators producing the dcP. There must be a dcP associated with the touch-dcMF, but it may be small and masked by other sources of dcP such as the sweat glands; because of their orientation, however, the sweat glands would produce no detectable dcMF to mask the follicle dcMF. We can support this by calculating an order-of-magnitude of the associated dcP. We assume the source to be a single dipole; from the maximal dcMF, this dipole would have a tangential component of 2.5 μA-cm. If it is located at 0.3 cm below the surface of a VC of 300 ohm-cm resistivity, and tilted at 45°, then the peak dcP on the surface would be $\approx$1.5 mV. This would be masked by the other dcPs that are >10 mV and explains why it has not been seen. Generally, however, any dcMF from the skin was unexpected. We had previously assumed that the high resistivity around any tangential sources in the skin would suppress their dcI and hence their dcMF. However, the scalp may be unique in this respect; it has both a lower resistivity (19) and a higher density of tangential sources (follicles) than any other skin area.

Because the dcMF over the forearms was absent over the atrophied forearms of the polio victims and present over the scar of a normal forearm, its source must intimately involve the muscles, not the skin. The nerve fibers for our purposes are similar to muscle fibers but of much smaller mass. We can assume that the dcMF over most other portions of the limbs is due to the same type of muscle source as in the forearms; the muscle fibers are similarly long and arranged longitudinally, and the dcMF levels are about the same. We suggest the following model for the production of dcMF by the limbs. The dcI is generated by nonuniform polarization along the long muscle fibers; there would be an associated variation in resting potential. This is due to the variation of extracellular K^+ concentration along the fibers (other ions can also be considered, but K^+ is the most active). This variation may result from enhanced K^+ outflow at the neuromuscular junction or from differences in K^+ diffusion and drainage. This model is supported by the injection data, in that the dcMF over the dog's thigh was seen to depend on muscle depolarization, hence nonuniformity along the muscle. More specifically, both the dog and human results are consistent with the Goldman equation, in which the depolarization emf is very sensitive to variation in K^+ but not in Na^+ concentration. Thus, in the equation, complete depolarization (emf change of 90 mV) is obtained by elevating K^+ concentration from about 3 to 165 mM; increasing K^+ further to 240 mM raises the emf change to about 110 mV, whereas 3 M yields 170 mV (polarization reversal). The time course in Fig. 4 suggests that the subcutaneous bolus needs some minutes to diffuse into the muscle, during which the dcMF rises. Then it decreases during the next 90 min with a time constant consistent with drainage times of alkali ions from muscle regions (21). The decreased dcMF from the deep injection is probably due to the closed, cancelling arrangement of depolarized fibers around the K^+ bolus, as opposed to a nonclosed bolus at the muscle surface.

Certainly the outstanding fact about the dcMF over the torso proper is the low level in comparison to the limbs; this may be fortunate in that it would allow any elevated dcMF from abnormal conditions in internal organs to be seen, such as injury currents from the heart (5). This low level is readily understood for areas of the torso devoid of extended semipermeable membranes, such as the female breast. For the muscular areas of the male torso this low level may be the result of muscle architecture. In contrast to limb muscles the torso muscles are much shorter and often arranged at an angle (bipennate or multipennate) in order to move with strength over short distances and probably have different drainage. These fibers may therefore not be exposed to large K^+ gradients, even from K^+ injection, and hence may not develop nonuniform polarization with resulting dcI and dcMF.

The authors thank the many subjects for their time and cooperation, Dr. Eugene Lepeschkin for his many excellent suggestions, and Dr. Richard Wilson for his help concerning breast tumors. This work was supported by Research Grants DAR76-19019 from the National Science Foundation and CA20631 from the National Institutes of Health.

1. Baule, G. & McFee, R. (1965) *J. Appl. Phys.* **36**, 2066–2073.
2. Cohen, D. (1975) *IEEE Trans. Magn.* **11**, 694–700.
3. Zimmerman, J. E. & Frederick, N. V. (1971) *Appl. Phys. Lett.* **19**, 16–19.
4. Cohen, D. (1969) *J. Appl. Phys.* **40**, 1046–1048.
5. Savard, P. & Cohen, D. (1979) *Digest of 12th International Conference on Medical and Biological Engineering (Jerusalem)* (Beilinson Medical Center, Petah Tikva, Israel), paper 36.5.
6. Cohen, D. & Givler, E. (1972) *Appl. Phys. Lett.* **21**, 114–116.
7. Karp, P. J., Katila, T. E., Mäkipää, P. & Saar, P. (1976) *Digest of 11th International Conference on Medical and Biological Engineering (Ottawa)* (National Research Council, Ottawa, Canada), pp. 504–505.
8. Cohen, D. & Hosaka, H. (1976) *J. Electrocardiol. (San Diego)* **9**, 409–417.
9. Grynszpan, F. & Geselowitz, D. B. (1973) *Biophys. J.* **13**, 911–925.
10. Plonsey, R. (1969) *Bioelectric Phenomena* (McGraw-Hill, New York), p. 152.
11. Plonsey, R. (1969) *Bioelectric Phenomena* (McGraw-Hill, New York), p. 98.
12. Plonsey, R. (1969) *Bioelectric Phenomena* (McGraw-Hill, New York), p. 56.
13. Plonsey, R. (1969) *Bioelectric Phenomena* (McGraw-Hill, New York), pp. 230–233.
14. Palti, Y., Gold, R. & Stämpfli, R. (1979) *Biophys. J.* **25**, 17–31.
15. Kidd, W. (1903) *The Direction of Hair in Animals and Man* (Adams & Charles Black, London).
16. Parnell, J. P. (1951) *Ann. N.Y. Acad. Sci.* **53**, 493–497.
17. Edelberg, R. (1973) *J. Appl. Physiol.* **34**, 334–340.
18. Montagna, W. & Ellis, R. A. (1958) in *The Biology of Hair Growth*, eds. Montagna, W. & Ellis, R. A. (Academic, New York), pp. 224–226.
19. Picton, T. W. & Hillyard, S. A. (1972) *Electroencephalogr. Clin. Neurophysiol.* **33**, 419–424.
20. Sano, K., Miyake, H. & Mayanagi, Y. (1967) *Electroencephalogr. Clin. Neurophysiol.*, Suppl. 25, 264–275.
21. Lassen, N. A. (1964) *J. Clin. Invest.* **43**, 1805–1812.